Analysis and Design of ICF Target Development Facility First Wall Reinforcing Structures

R.L. Engelstad and E.G. Lovell

July 1982

UWFDM-478

FUSION TECHNOLOGY INSTITUTE

UNIVERSITY OF WISCONSIN

MADISON WISCONSIN

Analysis and Design of ICF Target Development Facility First Wall Reinforcing Structures

R.L. Engelstad and E.G. Lovell

Fusion Technology Institute
University of Wisconsin
1500 Engineering Drive
Madison, WI 53706

http://fti.neep.wisc.edu

July 1982

UWFDM-478

ANALYSIS AND DESIGN OF ICF TARGET DEVELOPMENT FACILITY
FIRST WALL REINFORCING STRUCTURES

R.L. Engelstad

E.G. Lovell

Fusion Engineering Program
Nuclear Engineering Department
University of Wisconsin-Madison
Madison, WI 53706

July 1982

UWFDM-478

Abstract

Light ion beam inertial confinement fusion reaction vessels will be subjected to intense dynamic overpressure and heat flux from nuclear microexplosions. The conceptual design proposed consists of a cylindrical chamber with capped ends. The shell structure is supported by a gridwork of stringers and ribs. Modal static deflections and stresses for beam components are developed in parametric form. The dependence of modal dynamic load factors upon the pulse shape of the fireball blast wave are identified. Maximum dynamic load factor values are determined and characterized as functions of flexural frequencies for the structural components. The dynamic response is determined by coupling the static results with the appropriate dynamic load factors.

1. Introduction

One of the major influences on the mechanical design of ICF reaction chambers is the shock wave generated by the fireball. The shock wave imparts a dynamic pressure to the first wall which is assumed to be uniformly distributed over the surface. The reaction chamber considered for the Light Ion Beam Target Development Facility (TDF) is shown in Fig. 1.[1]

If the first wall structure is modeled as a perfect isolated thin cylindrical shell, then the radial pressure distribution will be sustained by uniform circumferential normal stress. In other words, such a concept is essentially a thin-walled tube in which the pressure generates circumferential stresses and complimentary axial normal stresses. Accounting for distributed mass and elasticity for this model will lead to dynamic response characterized by a breathing mode in which each cross section remains circular, expanding and contracting in simple harmonic motion following the mechanical shock.

However, such an idealized state will not be realized in an actual chamber because of a variety of mechanical constraints including beam ports and external supports. A practical design would use a shell with a structural reinforcement system. Since the overall shape of the TDF is cylindrical, a configuration with axial stringers and circumferential ribs is consistent. This is shown schematically in Fig. 1.

In the analysis which follows, the frame is modeled as a system of beams in which the curvature and hoop force capacity of the ribs are not included. In addition, the shell is assumed to transmit the full strength of the overpressure to the frame. This approach will lead to conservative design.

2. Dynamic Load Factor

One approach to the dynamic analysis of beams consists of determining the quasi-static reaction and multiplying it by a dynamic load factor (DLF) to

LIGHT ION BEAM TARGET DEVELOPMENT FACILITY

PRE-CONCEPTUAL DESIGN

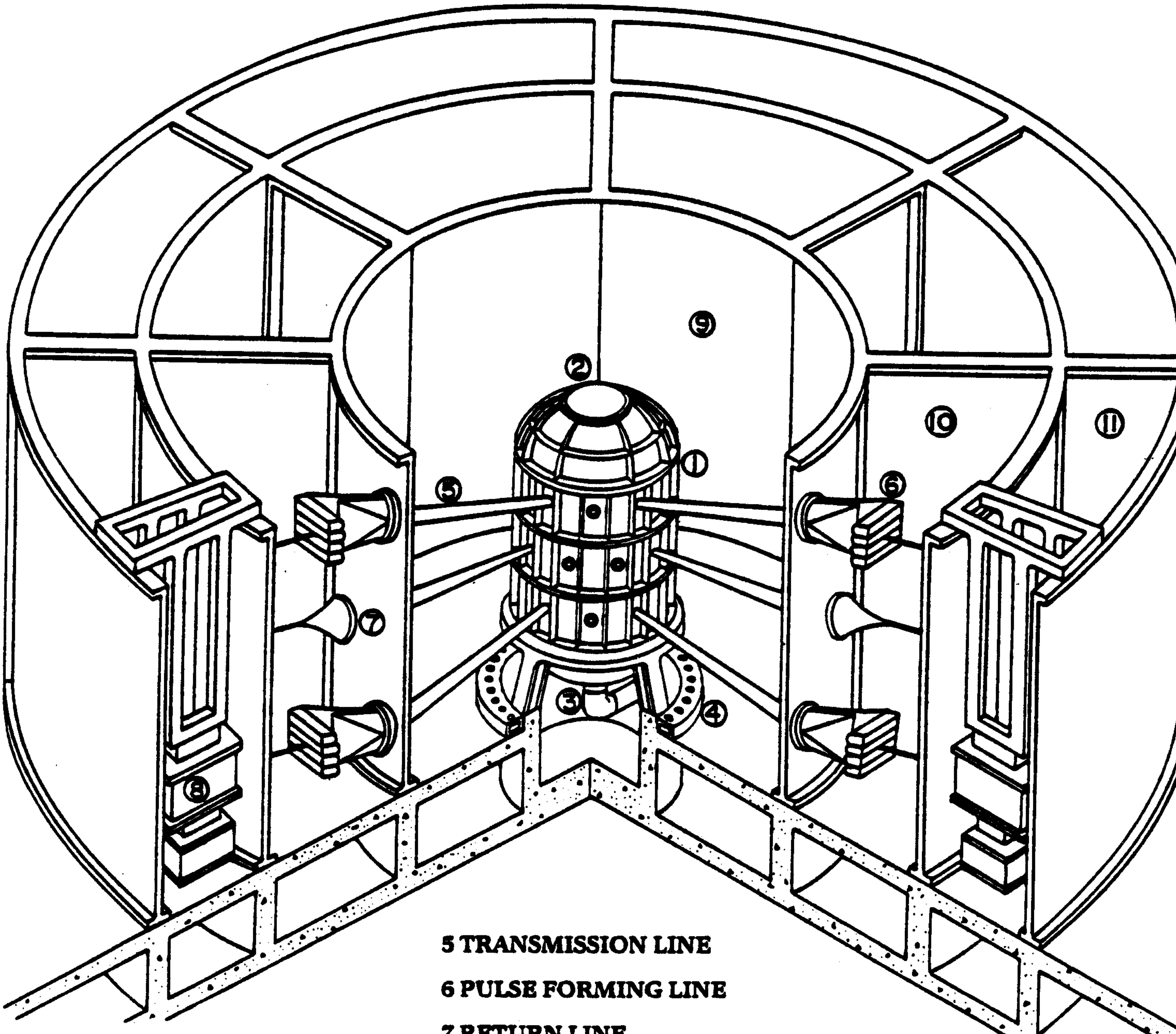

1 TARGET CHAMBER
2 DIAGNOSTIC PORT
3 PURGE LINE
4 AIR BUBBLE PLENUM
5 TRANSMISSION LINE
6 PULSE FORMING LINE
7 RETURN LINE
8 BEAM MARX GENERATOR
9 SHIELDING POOL - WATER
10 PULSE FORMING SECTION - WATER
11 ENERGY STORAGE SECTION - OIL

Figure 1

give corresponding dynamic effects. The dynamic load factor represents the ratio of the maximum dynamic response to the static response.[2]

Since a beam under uniform pressure will respond approximately as a single-degree-of-freedom system, it is appropriate to consider the dynamic response of such a system. For a simple spring-mass-damper system with forcing function F(t), the equation of motion is given by

$$m\ddot{y} + \bar{k}y + c\dot{y} = F(t) \tag{1}$$

where m and $\bar{k}$ are the mass and stiffness, respectively, and $c\dot{y}$ is the viscous damping force. To express the solution in parametric form it is convenient to introduce the concept of critical damping. This is the amount of damping that is needed to eliminate vibration and is defined as $c = \sqrt{\bar{k}m}$.

Considering free vibration, the homogeneous solution to the equation of motion is

$$y_H = e^{-\beta t} \left(C_1 \sin \omega_d t + C_2 \cos \omega_d t\right) \qquad \beta \leqslant \omega \tag{2}$$

where $\beta = c/2m$ and $\omega_d = \sqrt{\omega^2 - \beta^2}$. Here ω_d and ω represent the damped and undamped natural frequencies, respectively. If the system is subjected to an initial displacement and velocity, y_0 and $\dot{y}_0$, Eq. (2) becomes

$$y_H = e^{-\beta t} \left(\frac{\dot{y}_0 + \beta y_0}{\omega_d} \sin \omega_d t + y_0 \cos \omega_d t\right) . \tag{3}$$

It is apparent that when $\beta = \omega$ the response is no longer periodic. Instead of vibrating, the system simply returns to its equilibrium position, i.e. it is critically damped. Thus, β is a measure of the damping present and is specified as a certain percentage of the critical value.

For the forced response, consider the general load-time function shown in Fig. 2. The shaded area represents an impulse applied at time $t = \tau$. The particular solution for the forced vibration due to an increment of impulse is given by

$$y_P = \frac{F(\tau)\ d\tau}{m\omega_d} e^{-\beta(t-\tau)} \sin \omega_d(t - \tau) \ . \tag{4}$$

With $F(\tau) = F_{max}\ f(\tau)$, the static response is

$$y_{st} = F_{max}/\ \overline{k} = F_{max}/m\omega^2 \ . \tag{5}$$

This is substituted into Eq. (4) and the effects of all contributions are summed:

$$y_P = y_{st} \frac{\omega^2}{\omega_d} \int_o^t f(\tau)\ e^{-\beta(t-\tau)} \sin \omega_d(t - \tau)\ d\tau \ . \tag{6}$$

Finally, the complete solution is given by

$$y = y_H + y_P$$

or,

$$y = e^{-\beta t} \left(\frac{\dot{y}_o + \beta y_o}{\omega_d} \sin \omega_d t + y_o \cos \omega_d t\right) + y_{st} \frac{\omega^2}{\omega_d} \int_o^t f(\tau)\ e^{-\beta(t-\tau)} \sin \omega_d(t - \tau)\ d\tau \ . \tag{7}$$

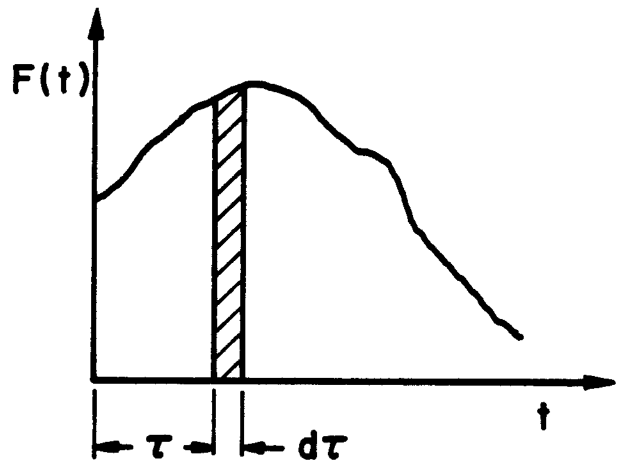

Figure 2

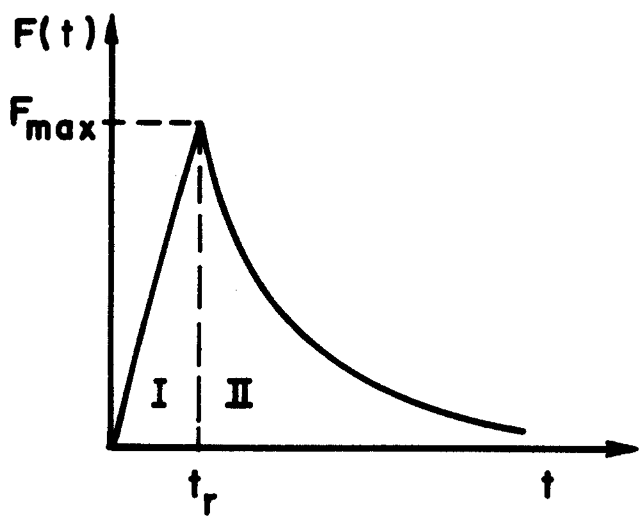

INTERVAL I: $f(\tau) = \frac{\tau}{t_r}$

INTERVAL II: $f(\tau) = e^{-k(\tau - t_r)}$

Figure 3

For the chamber wall design, a pressure-blast pulse is used for $f(\tau)$. The load function consists of a ramp with rise time t_r followed by an exponential function with decay constant k (Fig. 3). For the first interval the initial displacement and velocity are zero. Using DLF = y/y_{st} and integrating the response, the dynamic load factor for $t < t_r$ becomes

$$DLF = \frac{\omega^2}{t_r}\left[\frac{t}{\beta^2 + \omega_d^2} - \frac{2\beta}{(\beta^2 + \omega_d^2)^2} + \frac{e^{-\beta t}\{(\beta^2 - \omega_d^2)\sin\omega_d t + 2\beta\omega_d\cos\omega_d t\}}{\omega_d(\beta^2 + \omega_d^2)^2}\right] . \quad (8)$$

For the second interval y_0 and $\dot{y}_0$ are the displacement and velocity terms at $t = t_r$:

$$y_0 = \frac{\omega^2}{t_r}\left[\frac{t_r}{\beta^2 + \omega_d^2} - \frac{2\beta}{(\beta^2 + \omega_d^2)^2} + \frac{e^{-\beta t_r}\{(\beta^2 - \omega_d^2)\sin\omega_d t_r + 2\beta\omega_d\cos\omega_d t_r\}}{\omega_d(\beta^2 + \omega_d^2)^2}\right] \quad (9)$$

$$\dot{y}_0 = \frac{\omega^2}{t_r}\left[\frac{1}{\beta^2 + \omega_d^2} - \frac{\beta e^{-\beta t_r}\{(\beta^2 - \omega_d^2)\sin\omega_d t_r + 2\beta\omega_d\cos\omega_d t_r\}}{\omega_d(\beta^2 + \omega_d^2)^2} + \frac{e^{-\beta t_r}\{(\beta^2 - \omega_d^2)\cos\omega_d t_r - 2\beta\omega_d\sin\omega_d t_r\}}{(\beta^2 + \omega_d^2)^2}\right] . \quad (10)$$

Thus, the dynamic load factor for interval II ($t > t_r$) is

$$DLF = e^{-\beta(t-t_r)}\left[\frac{\dot{y}_0 + \beta y_0}{\omega_d}\sin\omega_d(t - t_r) + y_0\cos\omega_d(t - t_r)\right.$$
$$\left. + \frac{\omega^2}{\omega_d^2}\frac{e^{-\beta(t-t_r)}}{(\beta - k)^2 + \omega_d^2}\left[\omega_d e^{(\beta-k)(t-t_r)} - (\beta - k)\sin\omega_d(t - t_r) - \omega_d\cos\omega_d(t - t_r)\right]\right. . \quad (11)$$

3. Frame Analysis

The dynamic overpressure is considered uniform over the plates and partitioned to the stringers and ribs as shown in Fig. 4. The tributary areas will

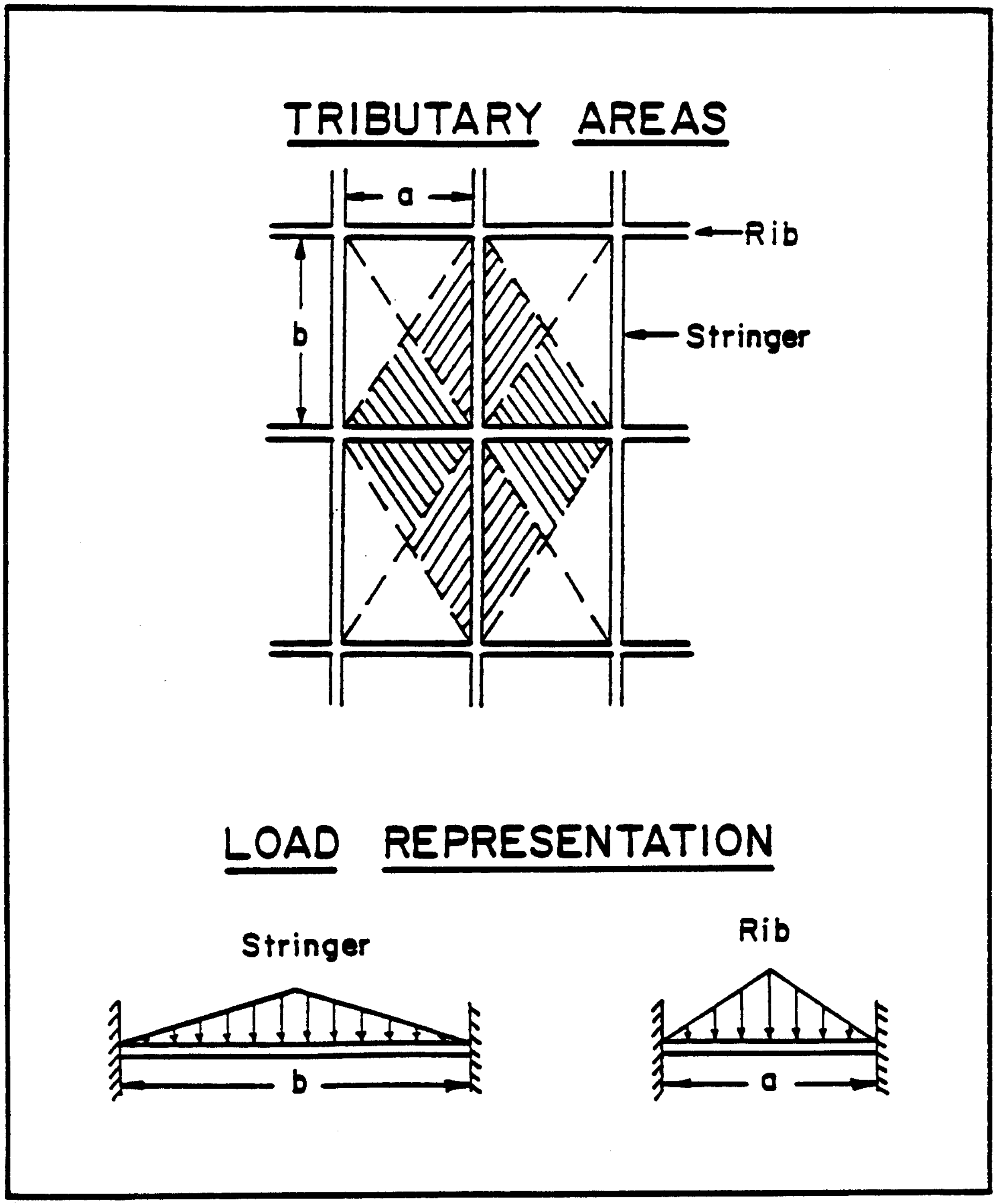
TRIBUTARY AREAS
a
Rib
b
Stringer
LOAD REPRESENTATION
Stringer
b
Rib
a

Figure 4

produce uniformly varying line loads with maximum values pa and pb for stringers and ribs, respectively, where p denotes the maximum overpressure from the shock. The procedure for analyzing the stringers and ribs involves first determining the static response and subsequently modifying this by means of a dynamic load factor to account for dynamic effects.[3] In this case, stringer and rib lengths have been chosen a priori. The design effort primarily involves the determination of cross section characteristics such that the mechanical stresses are within design limits and deflections are not excessive.

The analysis uses a prismatic beam element with uniform mass per unit length under a time-dependent loading which may be arbitrarily distributed but is eventually specialized to the profile shown in Fig. 4. The effects of shear deformation and rotary inertia are not included. With these considerations, then, the principal equation of motion governing the transverse vibration of the beam is given by

$$EI \frac{\partial^4 y(x,t)}{\partial x^4} + \bar{m} \frac{\partial^2 y(x,t)}{\partial t^2} = p(x,t) \qquad (12)$$

where: E = elastic modulus

I = cross section moment of inertia

$\bar{m}$ = mass per unit length

p = dynamic pressure (force per unit length)

t = time

y = transverse displacement.

The coordinate system and loading on a typical beam of length ℓ are shown in Fig. 5.

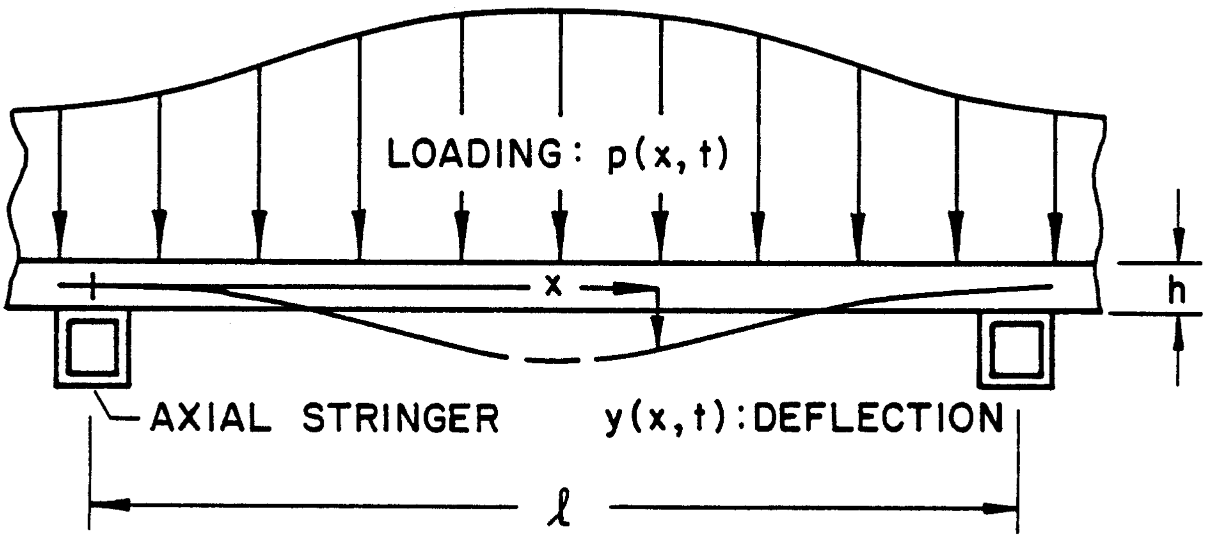

Figure 5

To determine the natural frequencies of the beam, the external load is set equal to zero, resulting in the differential equation for free vibration. A solution of the form

$$y(x,t) = \Phi(x)\ Y(t) \tag{13}$$

is substituted into Eq. (12), leading to

$$\frac{EI}{\bar{m}\Phi(x)} \frac{d^4\Phi(x)}{dx^4} = \frac{1}{Y(t)} \frac{d^2Y(t)}{dt^2} \ . \tag{14}$$

With x and t being independent variables, the preceding equation can be satisfied only if both sides are set equal to a constant, producing two ordinary differential equations. Choosing ω^2 for this constant, these equations will have solutions of the form

$$Y(t) = C_1 \sin \omega t + C_2 \cos \omega t \tag{15}$$

$$\Phi(x) = A\sin ax + B\cos ax + C\sinh ax + D\cosh ax \tag{16}$$

where

$$a^4 = \overline{m}\omega^2/EI \ .$$

The deformed shape of any span can be characterized by zero slope change and zero relative deflection at each end. Thus, the boundary conditions are

$$\begin{aligned} y(0,t) &= y(\ell,t) = 0 \\ \partial y(0,t)/\partial x &= \partial y(\ell,t)/\partial x = 0 \ . \end{aligned} \tag{17}$$

With these and Eq. (16) the following transcendental equation is obtained:

$$\cos a\ell \cosh a\ell = 1 \ . \tag{18}$$

This equation generates an infinite number of discrete eigenvalues, a_n ($n = 1,2,3,\ldots$), which are obtained numerically and are related to the natural frequencies ω_n by

$$\omega_n = a_n^2 (EI/\ \overline{m})^{1/2} \qquad\qquad n = 1,2,3,\ldots \tag{19}$$

Corresponding to each natural frequency is a characteristic shape or eigenfunction

$$\Phi_n(x) = C_n\ [(A_n/B_n)(\sinh a_n x - \sin a_n x) + \cosh a_n x - \cos a_n x] \tag{20}$$

where $A_n/B_n = (\cos a_n\ell - \cosh a_n\ell)/(\sinh a_n\ell - \sin a_n\ell)$

and C_n is an arbitrary constant.

After the mode shapes and frequencies have been determined, a modal-superposition method of analysis can be used to solve for the dynamic response of the forced vibration. Thus, any displacement can be expressed by superimposing appropriate amplitudes of the vibration mode shapes for the structure. This can be written as

$$y(x,t) = \sum_n \Phi_n(x)\, Y_n(t) \,. \qquad (21)$$

Using an energy solution, Lagrange's equation is applied to the system

$$d[\partial K/\partial \dot{Y}_n(t)]/dt + \partial U/\partial Y_n(t) = \partial \Omega_e/\partial Y_n(t) \qquad (22)$$

where: K = total kinetic energy

U = total flexural strain energy

Ω_e = external work

and $(\cdot)$ denotes differentiation with respect to time, t. The kinetic energy for the entire system is given by

$$\begin{aligned} K &= (1/2)\,\bar{m} \int_0^\ell \dot{y}(x,t)^2\, dx \\ &= (1/2)\,\bar{m} \int_0^\ell [\sum_n \Phi_n(x)\, \dot{Y}_n(t)]^2\, dx \qquad (23) \\ &= (1/2)\,\bar{m} \sum_n \dot{Y}_n^2(t) \int_0^\ell \Phi_n^2(x)\, dx \end{aligned}$$

where $\overline{m}$ is considered to be constant over the span and orthogonality of the mode shapes has been utilized.

The work done by external forces is

$$\Omega_e = \int_0^\ell p(x,t)\ y(x,t)\ dx$$

$$= \int_0^\ell p(x,t)[\sum_n \Phi_n(x)\ \dot{Y}_n(t)]\ dx\ . \qquad (24)$$

Considering $p(x,t) = P(x)f(t)$, where $P(x)$ is the spatial load distribution and $f(t)$ is the time function, the external work becomes

$$\Omega_e = f(t) \sum_n Y_n(t) \int_0^\ell P(x)\ \Phi_n(x)\ dx\ . \qquad (25)$$

Substituting into Eq. (22) yields

$$\overline{m}\ \ddot{Y}_n(t) \int_0^\ell \Phi_n^2(x)\ dx = \partial U/\partial Y_n(t) = f(t) \int_0^\ell P(x)\ \Phi_n(x)\ dx$$

or

$$\ddot{Y}_n(t) = \omega_n^2\ Y_n(t) = f(t) \int_0^\ell P(x)\ \Phi_n(x)\ dx/\ \overline{m} \int_0^\ell \Phi_n^2(x)\ dx\ . \qquad (26)$$

Eliminating the time dependency, the modal static deflection can be defined as follows:

$$Y_{n\ st} = \int_0^\ell P(x)\ \Phi_n(x)\ dx/\ \overline{m}\ \omega_n^2 \int_0^\ell \Phi_n^2(x)\ dx\ . \qquad (27)$$

To determine the dynamic response, the static response is multiplied by the dynamic load factor (DLF). Then, the total deflection at any point is given by

$$y(x,t) = \sum_n \Phi_n(x)\, Y_{n\,st}\, DLF_n \,. \tag{28}$$

The dynamic bending moment can be determined from

$$M(x,t) = EI\, \partial^2 y(x,t)/\partial x^2 = EI \sum_n Y_{n\,st}\, DLF_n\, d^2\Phi_n(x)/dx^2 \tag{29}$$

giving a flexural stress

$$\sigma(x,t) = M(x,t)h/2I = (h/2)E \sum_n Y_{n\,st}\, DLF_n\, d^2\Phi_n(x)/dx^2 \tag{30}$$

where h is the cross section depth of the beam (Fig. 5).

Equations (28) and (30) are used to determine the beam deflections and stresses, respectively. These equations can be simplified by considering P(x) to be uniformly varying line loads as shown in Fig. 4. Also, it is found in the beam analysis that the fundamental mode dominates both the static and dynamic response. Therefore, only the first mode will be considered in the following computations.

4. Quantitative Results

The reaction chamber (Fig. 1) has a cylindrical shell structure with a height and diameter of 6 meters. Since the 40 beam ports are located in planes at three elevations, it is convenient to partition the stringers and ribs into lengths of 200 cm and 47 cm, respectively.

A number of materials have been proposed for the chamber wall and it would be practical to use the same alloy for the stringers and ribs. Since these components are completely immersed in the shield water, the material properties correspond to 25°C.[4]

The dependence of stringer and rib fundamental frequencies on cross-sectional radius of gyration is shown in Fig. 6. It can be seen that the natural frequencies of the ribs are approximately an order of magnitude greater than those of the stringers. This is an important design consideration since dynamic load factors are strongly influenced by the flexural frequency magnitudes. The dynamic load factors also depend upon the shock ramp time (t_r) and the exponential decay coefficient (k).

The frame analysis was based on a specific fireball calculation that included the largest overpressure which could be expected in the TDF cavity gas. This corresponds to xenon cavity gas at 70 torr seeded with 0.5% Cs with a resulting maximum overpressure of 1.71 MPa at 1.32 ms (Fig. 7).(1) The coefficients t_r and k were determined to be 0.14 ms and 3432/s, respectively. Then, using Eqs. (8) and (11) numerical computations were carried out to obtain the maximum DLF as a function of the fundamental vibration frequency for various levels of damping as shown in Fig. 8. Because of the relatively low frequencies of the stringers, the DLF will generally be less than unity but the rib DLF's will be substantially larger.

Design curves for flexural stress as a function of cross section modulus for both stringers and ribs have been developed from Eq. (30). These curves represent the maximum static stress associated with the fundamental mode at the "fixed" end of the beam. The overpressures cover a range of values and include the specific case of 1.71 MPa as shown in Figs. 9 and 10. It should be noted that the stress graphs can be used for any elastic material under the given conditions. The design stress would be based upon both the yield characteristics of the material and the DLF. With this, the section modulus can be determined and thus the beam properties are established. In addition, static deflections for the first mode have been developed from Eq. (28).

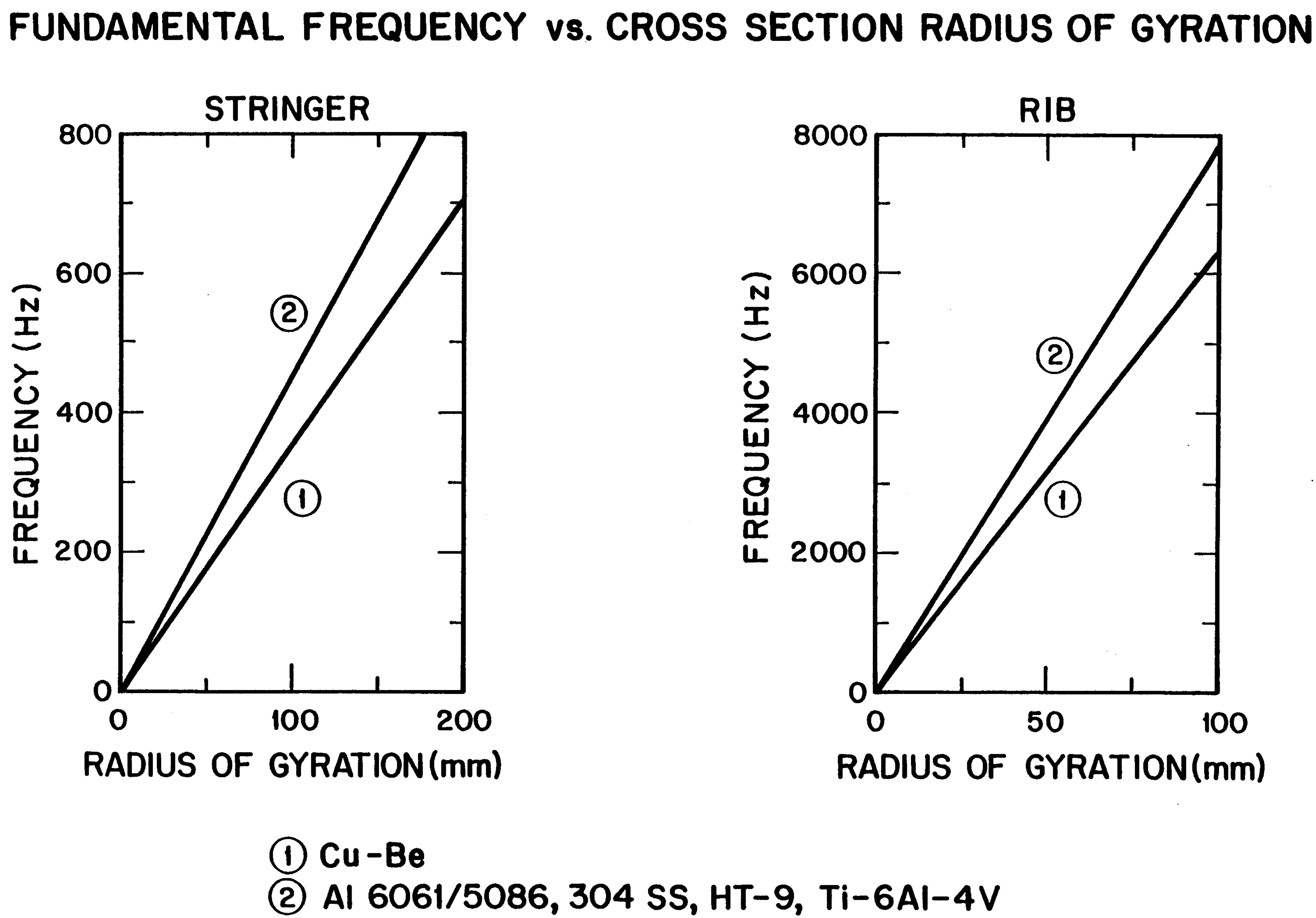
FUNDAMENTAL FREQUENCY vs. CROSS SECTION RADIUS OF GYRATION
STRINGER
FREQUENCY (Hz)
800
600
400
200
0
0
100
200
RADIUS OF GYRATION (mm)
②
①
RIB
FREQUENCY (Hz)
8000
6000
4000
2000
0
0
50
100
RADIUS OF GYRATION (mm)
②
①
① Cu-Be
② Al 6061/5086, 304 SS, HT-9, Ti-6Al-4V

Figure 6

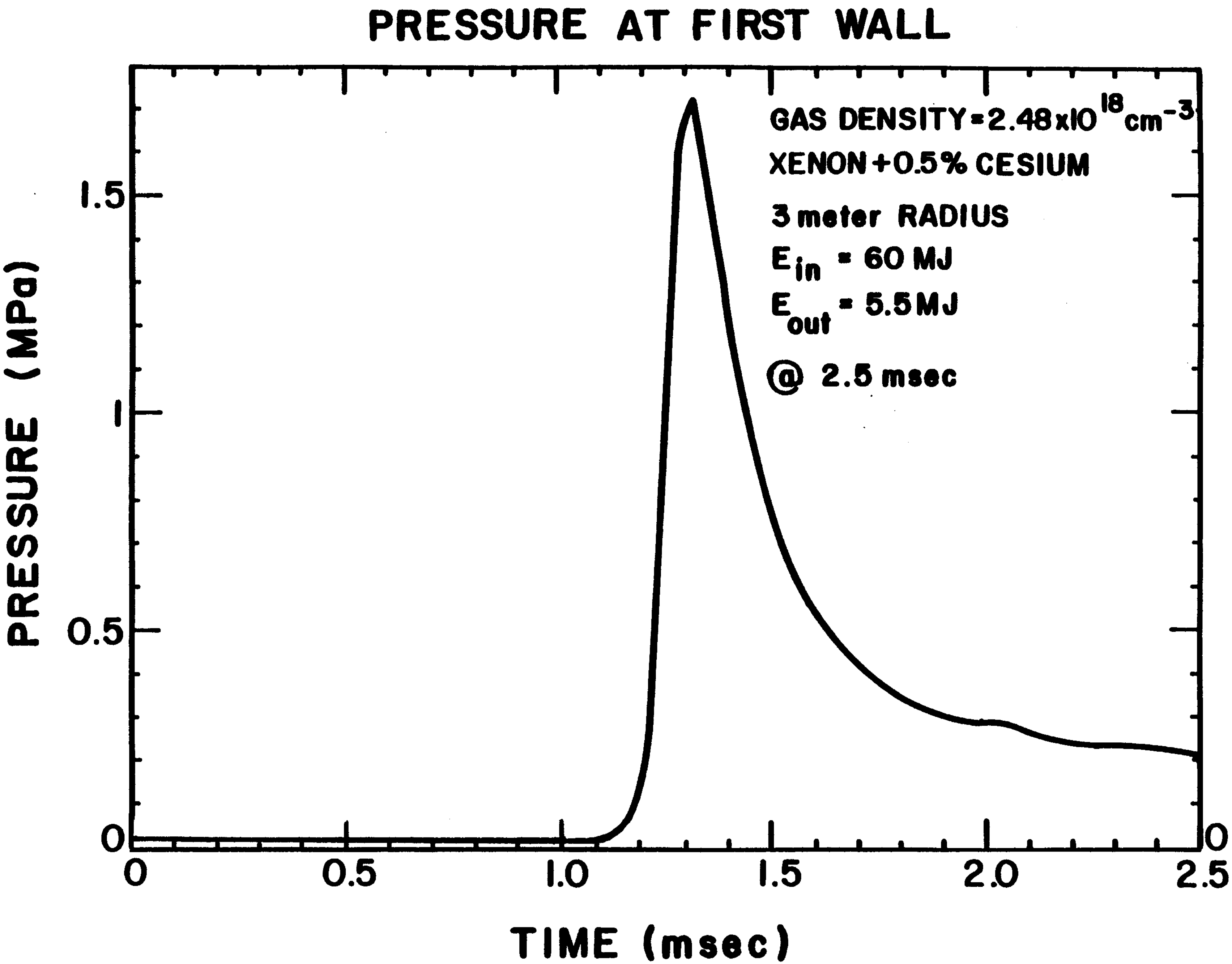
PRESSURE AT FIRST WALL
GAS DENSITY = 2.48x10^18 cm^-3
XENON + 0.5% CESIUM
3 meter RADIUS
E_in = 60 MJ
E_out = 5.5 MJ
@ 2.5 msec
PRESSURE (MPa)
TIME (msec)
0
0.5
1
1.5
1.0
2.0
2.5

Figure 7

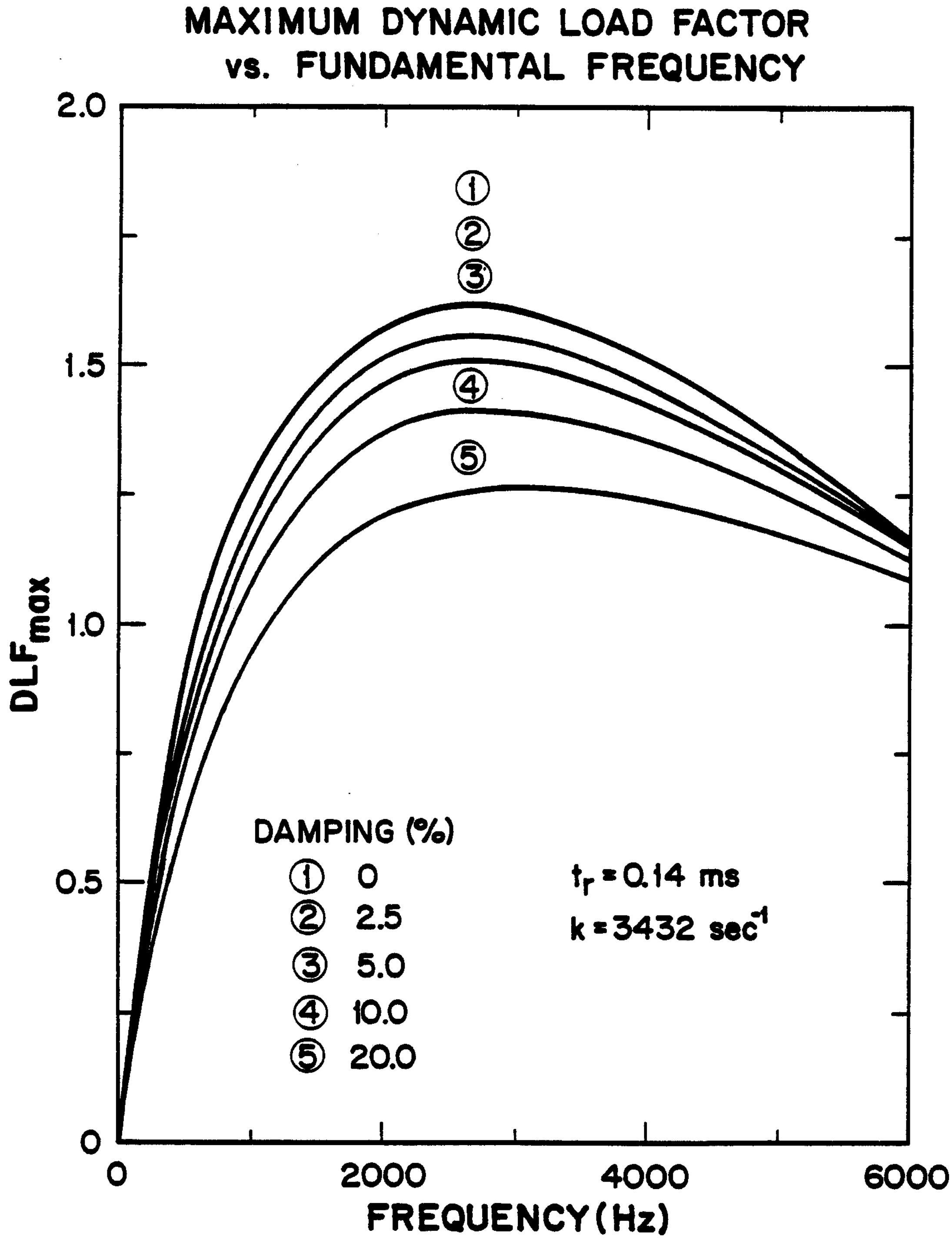
MAXIMUM DYNAMIC LOAD FACTOR
vs. FUNDAMENTAL FREQUENCY
2.0
1.5
1.0
0.5
0
DLFmax
①
②
③
④
⑤
DAMPING (%)
① 0
② 2.5
③ 5.0
④ 10.0
⑤ 20.0
tr = 0.14 ms
k = 3432 sec-1
0
2000
4000
6000
FREQUENCY (Hz)

Figure 8

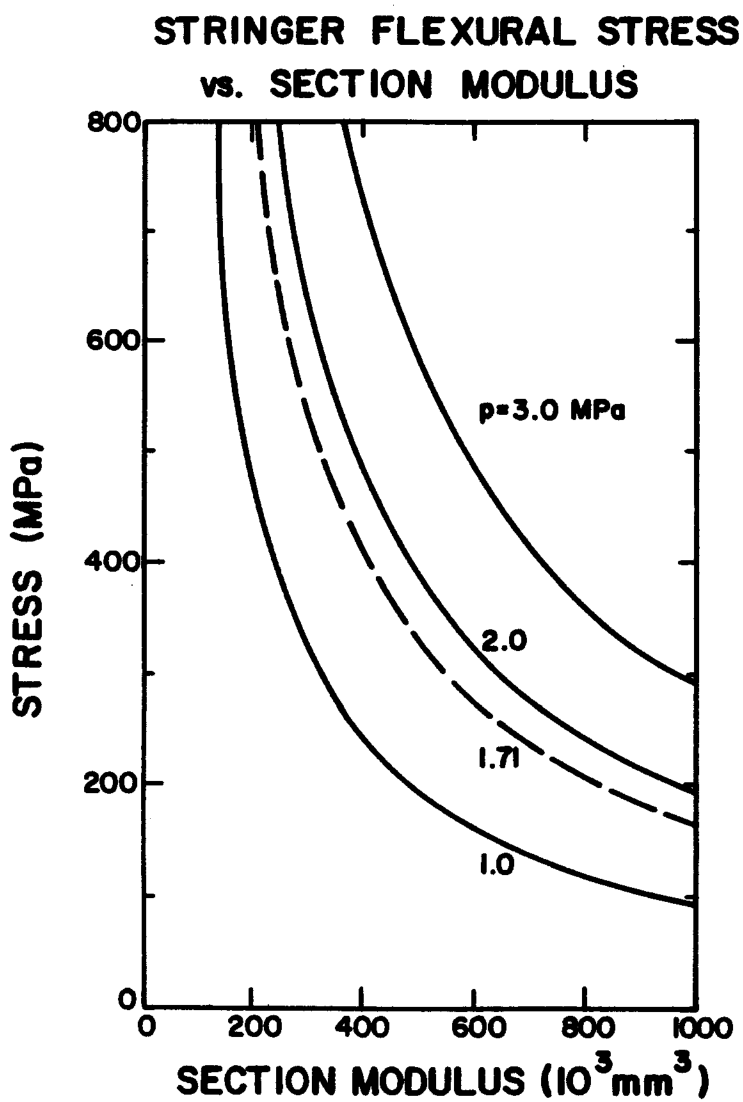

Figure 9

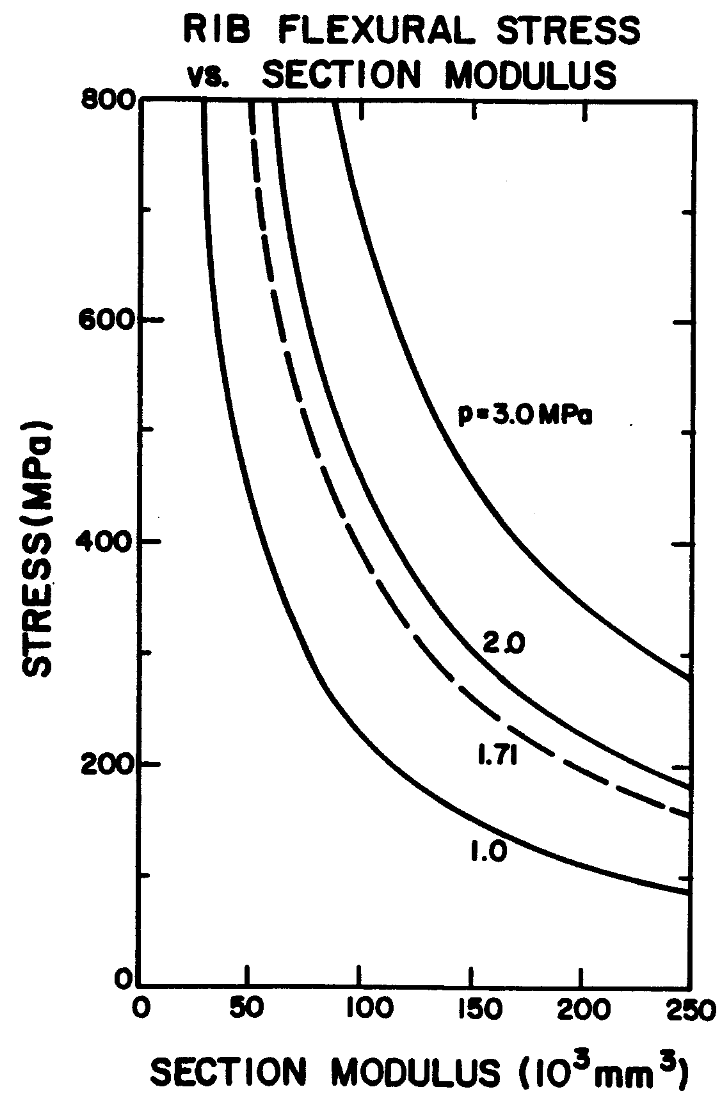

Figure 10

Figures 11-20 show the midspan displacement as a function of cross section moment of inertia for stringers and ribs for the various materials under consideration.

5. Numerical Example

A specific case is presented here to outline the procedure. The material selected is aluminum 6061 with a yield stress of 276 MPa. Cavity gas is xenon with 0.5% Cs and an overpressure of 1.71 MPa as indicated earlier. In this work, the following notation is used:

I = major axis moment of inertia

S = major axis section modulus

r = major axis radius of gyration

ω = fundamental flexural frequency

σ = flexural stress

y = maximum transverse displacement.

The various steps in the design procedure are summarized in Table 1. It can be seen that the AISC manual has first been used to select four different sizes of rectangular structural tubing. For each of these, the relevant cross section parameters are listed. Next, the fundamental frequency is determined and consequently the DLF is established. Using the cross section modulus (S) and moment of inertia, the static stress and deflection (σ_s and y_s) for each are found from the appropriate design curves. These in turn must be amplified by the DLF to give the corresponding dynamic response (σ_d and y_d). Finally, each dynamic result must be compared with the design limits.

From the sample calculations in the table it is observed that the stresses in the 8 inch tubing are below yield with acceptable deflections for both stringers and ribs. With these dimensions a section of the wall and frame has been drawn in proportion and is shown in Fig. 21.

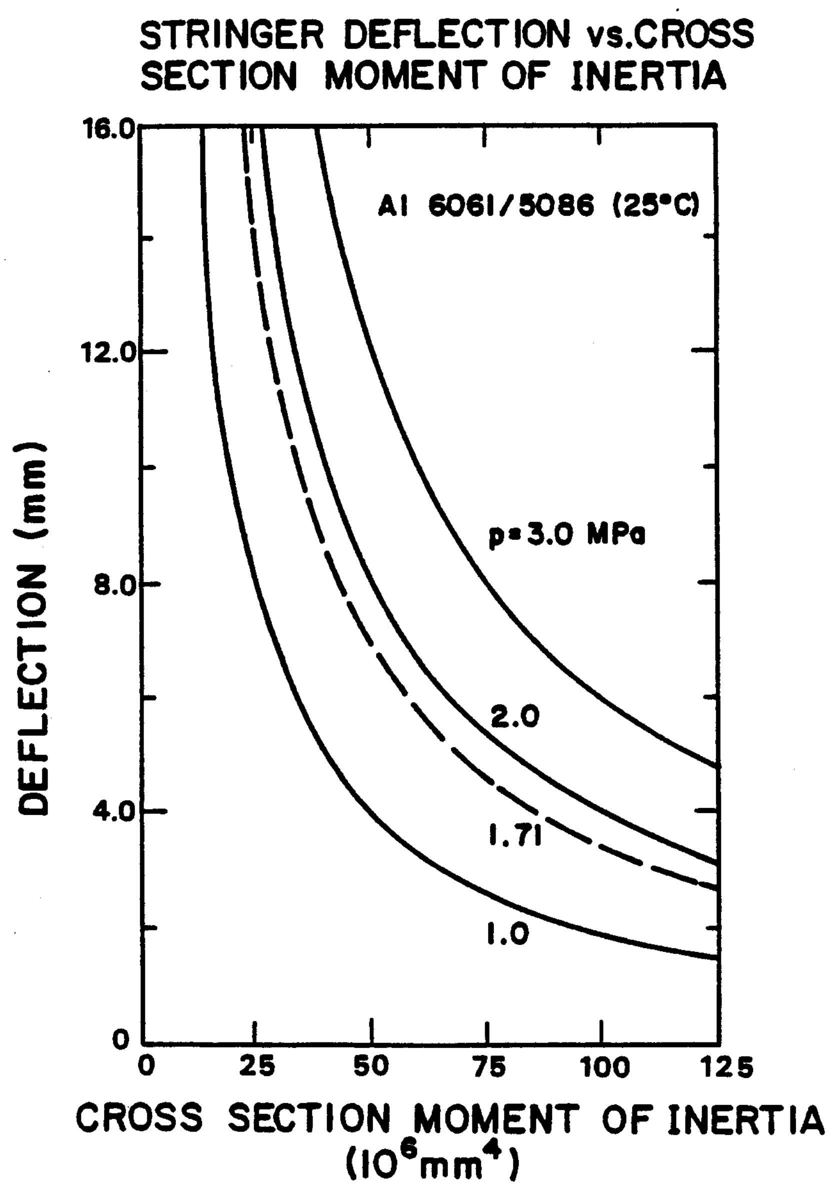

Figure 11

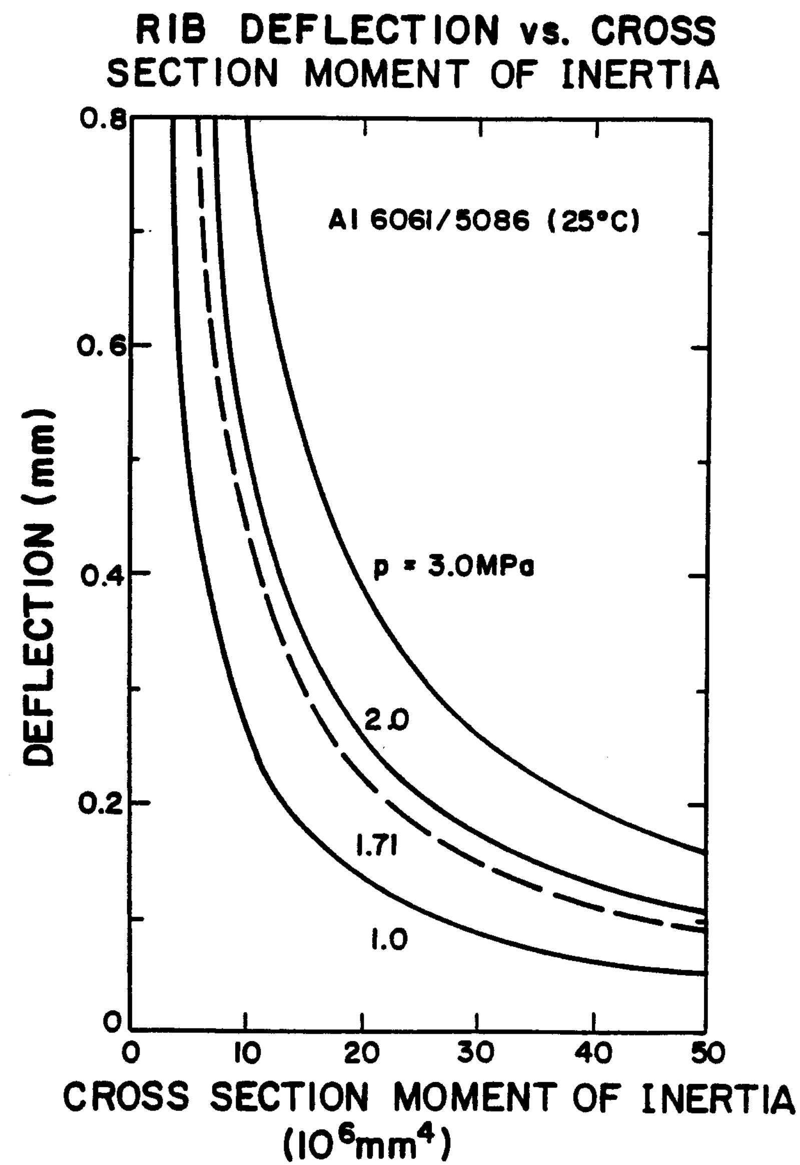

Figure 12

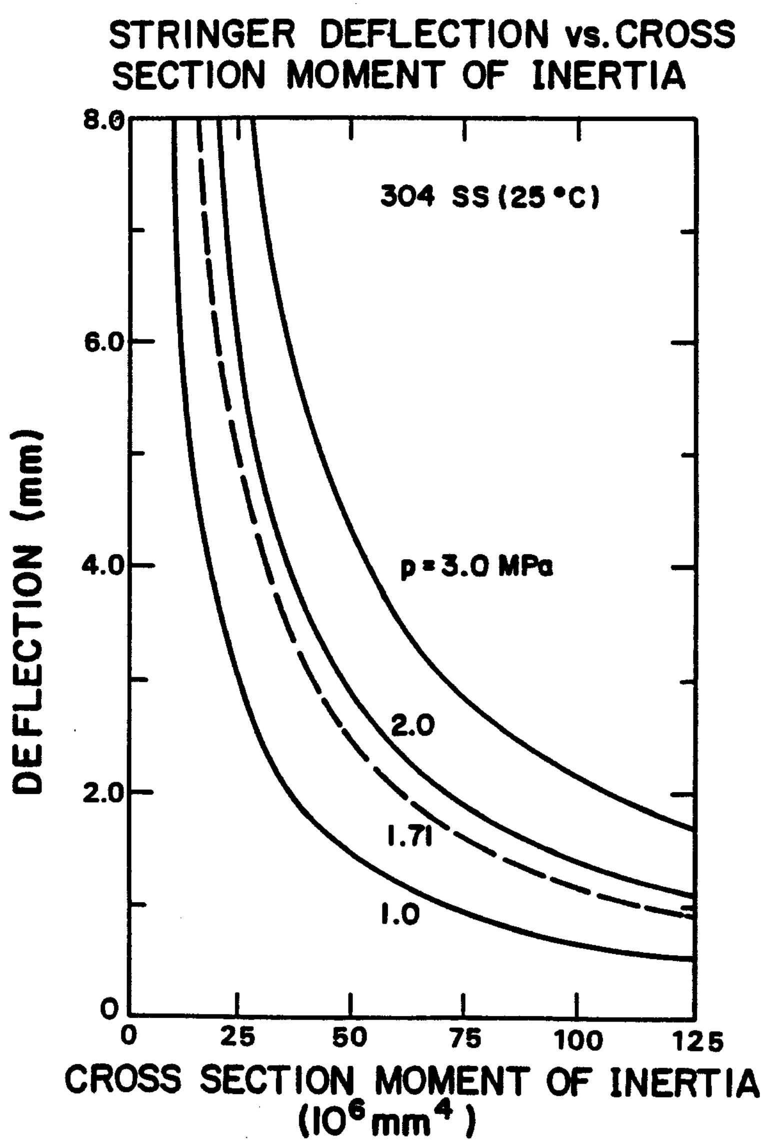

Figure 13

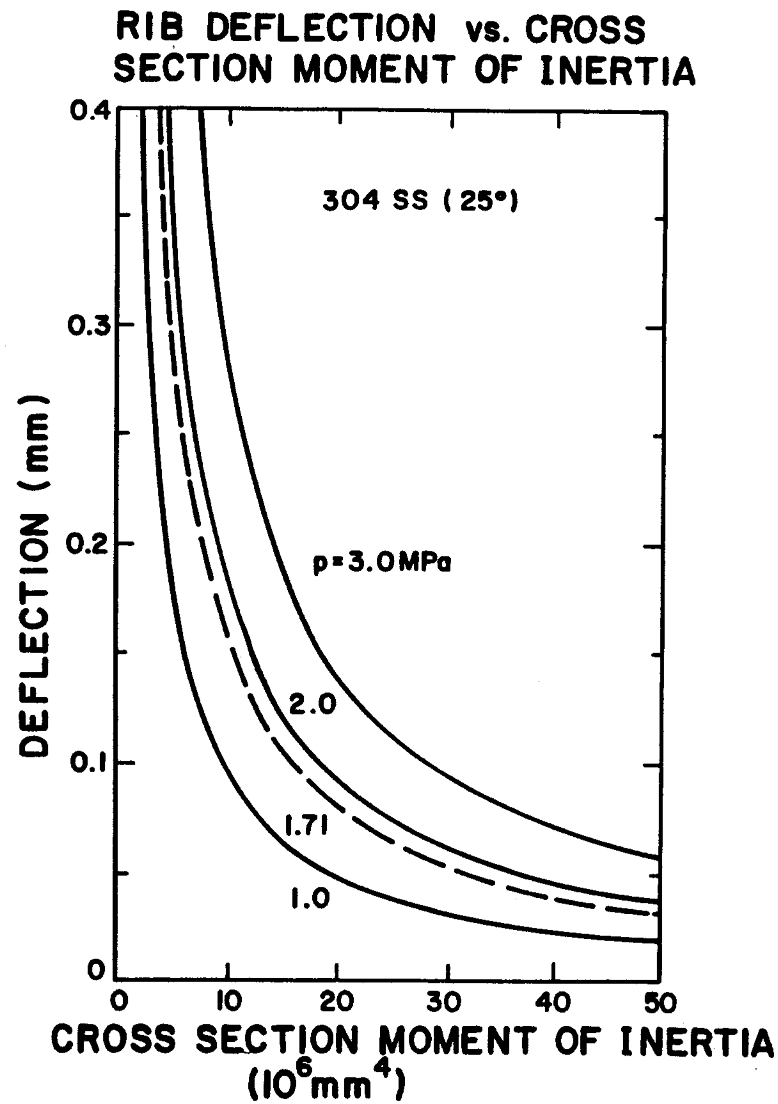

Figure 14

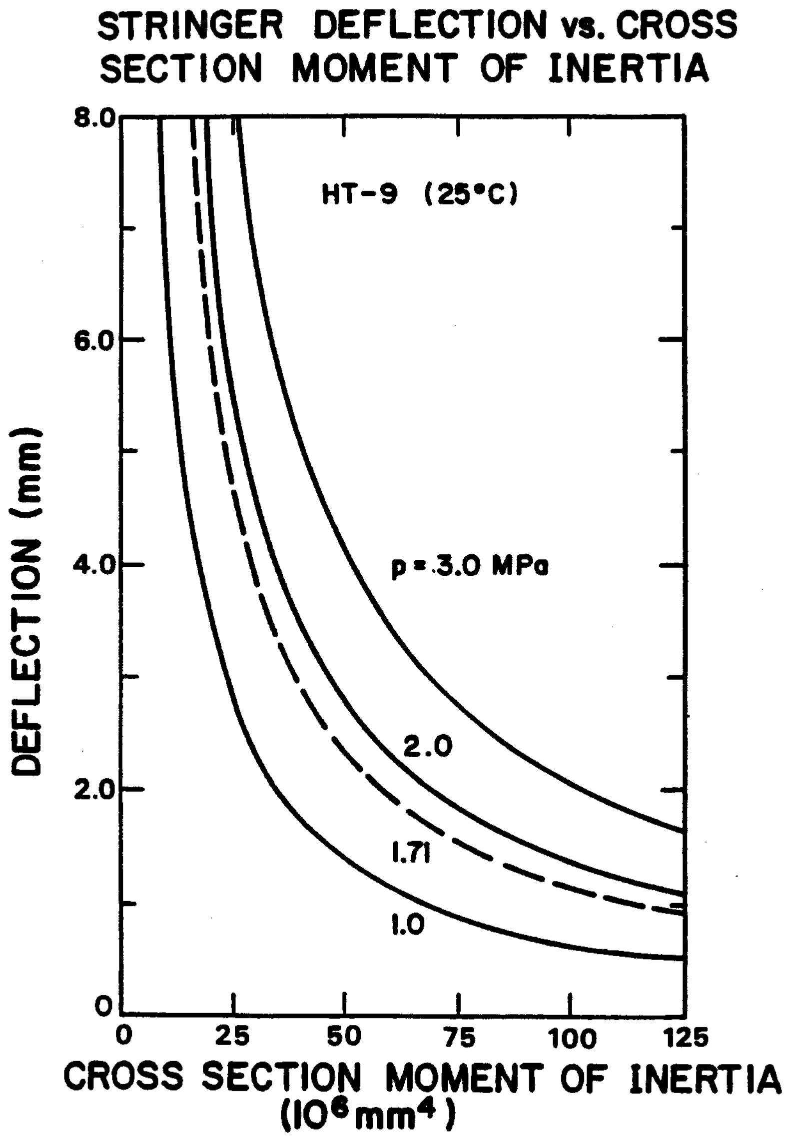

Figure 15

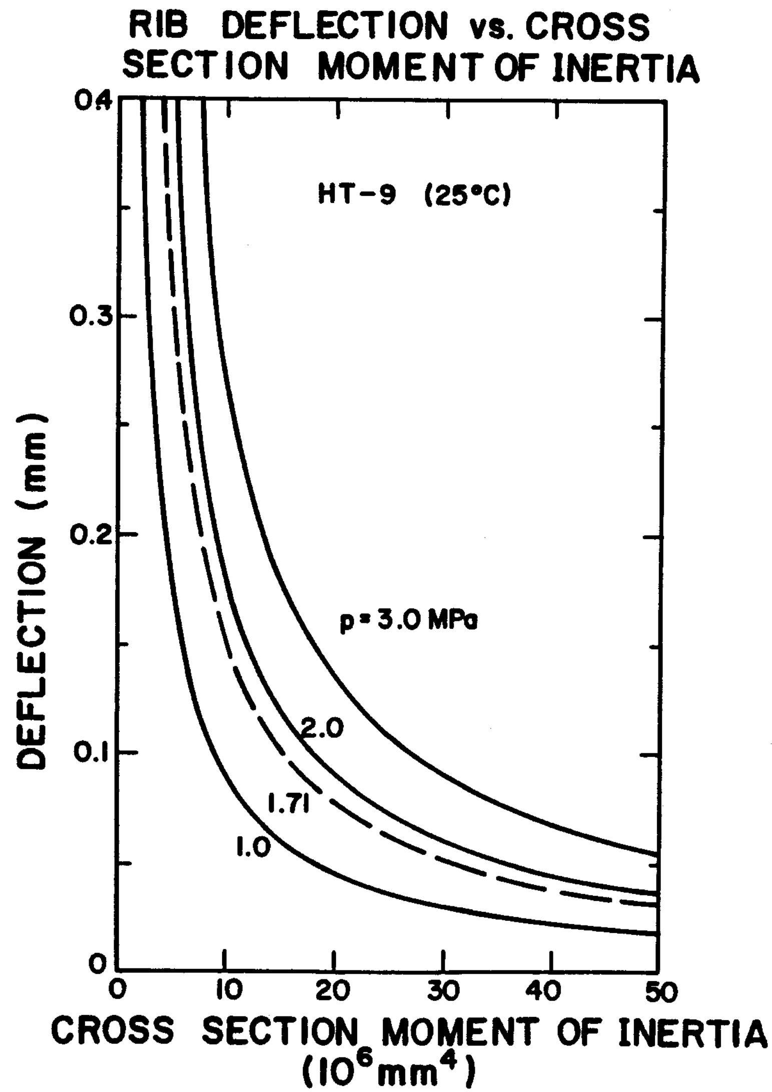

Figure 16

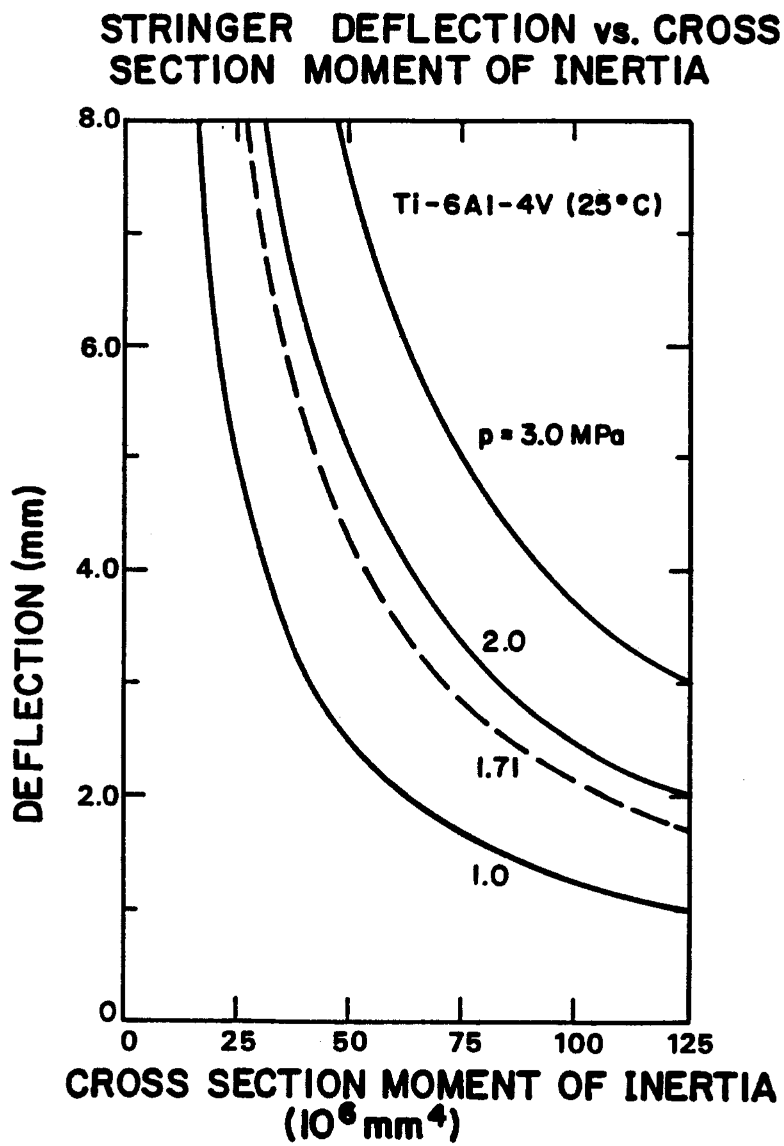

Figure 17

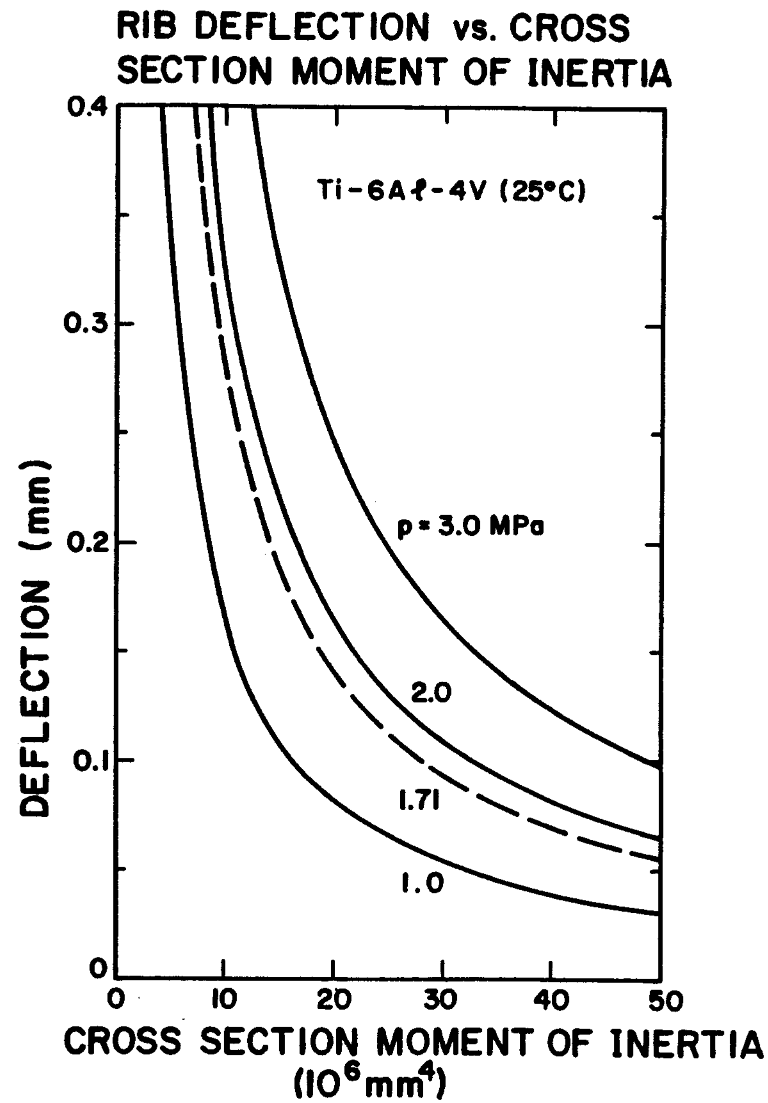

Figure 18

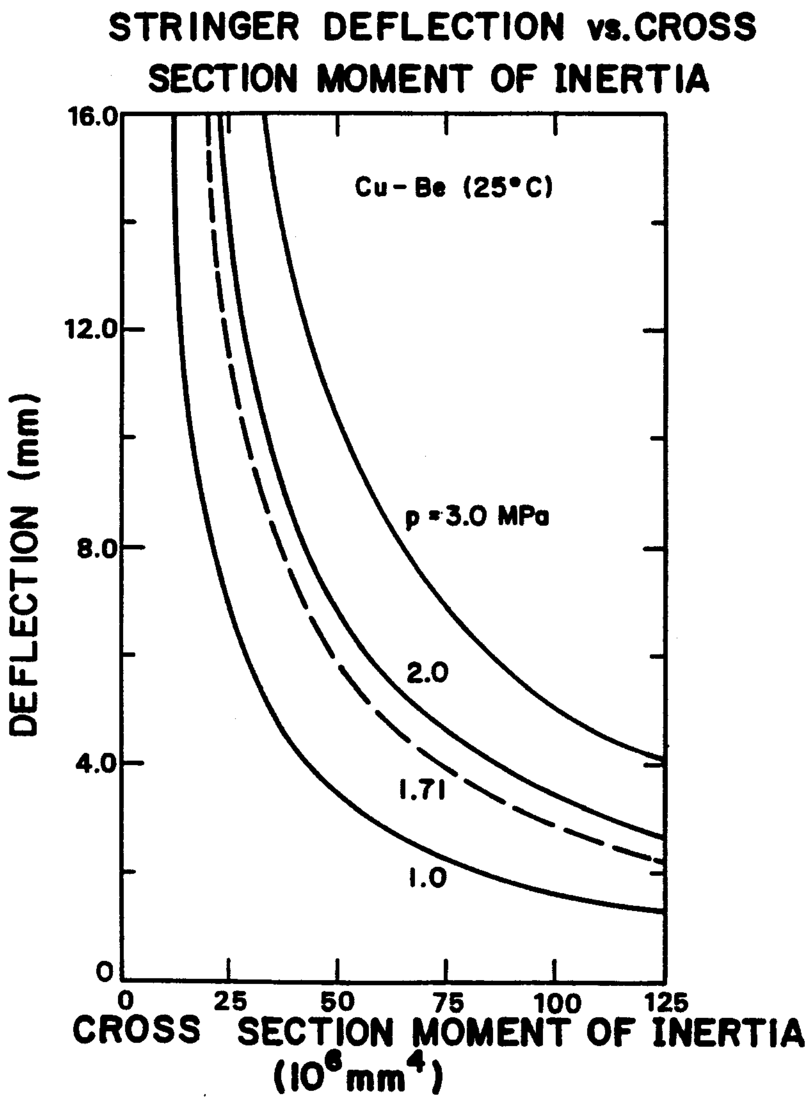

Figure 19

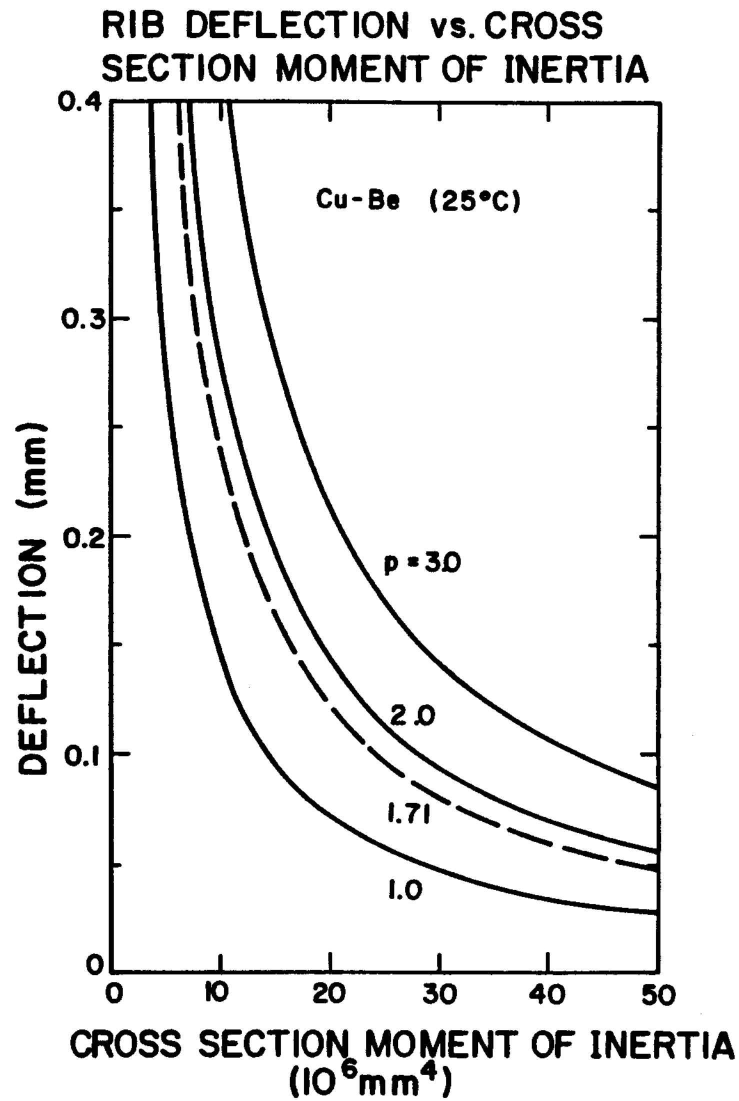

Figure 20

STRUCTURAL FRAME DESIGN EXAMPLE
Al 6061/5086; Overpressure 1.71 MPa

		STRINGER		RIB	
1. Structural Tubing Dimensions from AISC Manual (in.)		8x6x1/2	7x5x1/2	8x3x3/8	7x4x3/8
2. Cross Section Parameters from AISC Manual	I-in^4 ($10^6 mm^4$)	103.0 (42.9)	63.5 (26.4)	51.0 (21.2)	44.0 (18.3)
	S-in^3 ($10^3 mm^3$)	25.8 (422.8)	18.1 (296.6)	12.7 (208.1)	12.6 (206.5)
	r-in. (mm)	2.89 (73.4)	2.48 (63.0)	2.64 (67.0)	2.45 (62.2)
3. Static Response from Design Curves	ω-Hz	330	284	5465	5073
	DLF	0.65	0.58	1.27	1.34
	σ_s-MPa	391	558	187	189
	y_s-mm	7.94	12.9	0.21	0.24
4. Dynamic Response (Undamped)	σ_d-MPa	254	324	238	253
	O.K.?	Yes	No	Yes	Yes
	y_d-mm	5.16	7.5	0.27	0.32
	O.K.?	Yes	Yes	Yes	Yes

Table 1

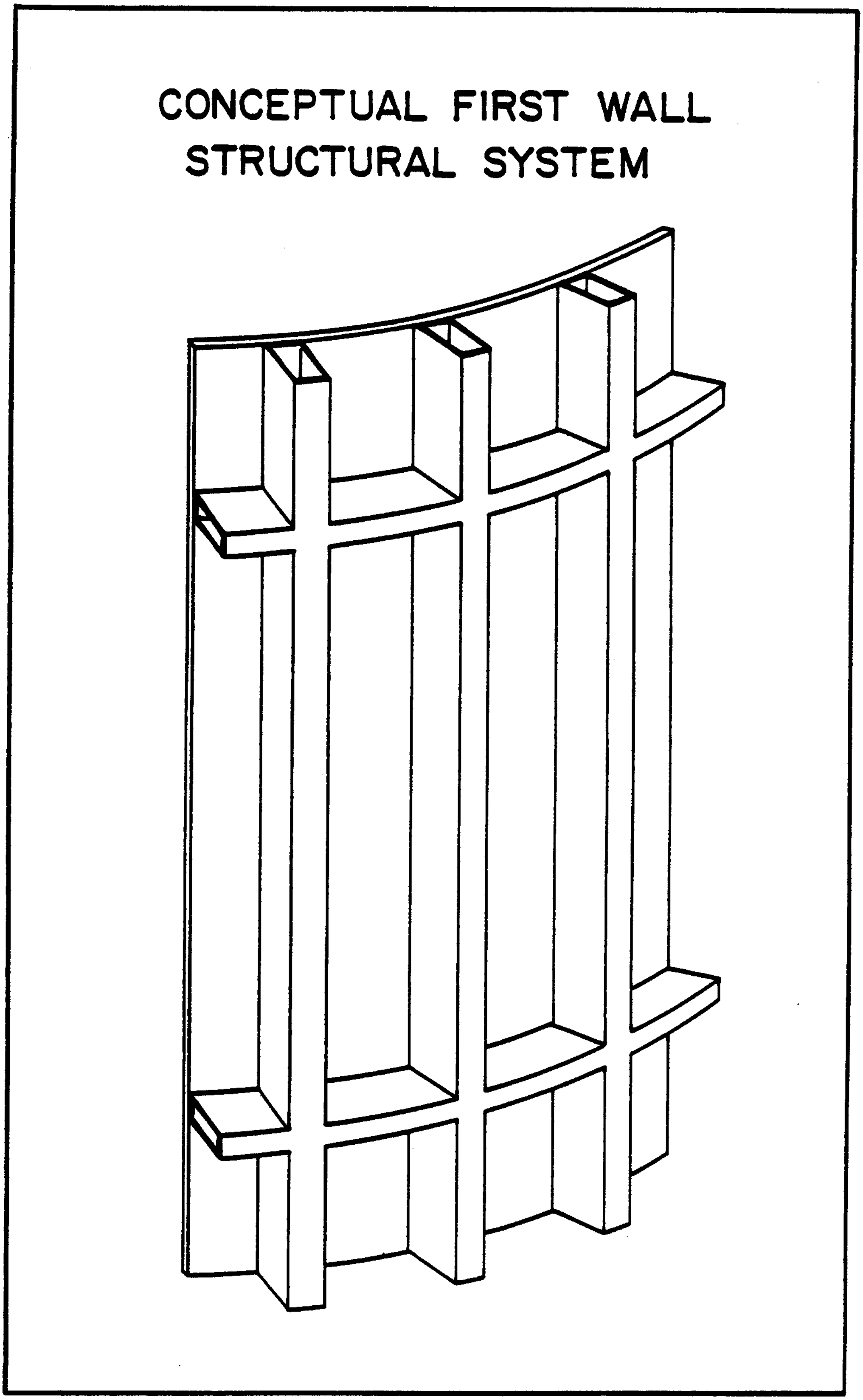

Figure 21

Stress and deflection time histories have also been determined. For example, the flexural stress response of both the stringers and ribs are shown in Figs. 22-25. In the undamped cases it can be seen that initially the stress response follows the pulse and subsequently develops into free vibration. With damping the number of cycles at various stress levels can be determined and subsequently used in fatigue life calculations.

This specific example is intended to identify the details of the design procedure. Different aspect ratios for the stringer and rib spacings can be used. As well, different geometries for the stringer and rib cross sections can be considered. Finally it should be emphasized that the analysis upon which the design procedure is based is extremely conservative. Refinements will lead to a design in which stringers and ribs are both lighter and not as closely spaced.

6. Conclusions

Modal analysis has been used to determine the response of reaction chamber reinforcement components proposed for a light ion fusion target development facility. From the techniques developed, parametric data is generated for design purposes. The relationship is established between stress and deflection magnitudes and extreme values of dynamic load factors. These in turn are shown to be primarily dependent on the natural frequencies of the components, structural damping levels, and the shape and amplitude of the dynamic overpressure. In particular, it is shown that the supporting structure can be designed to carry the dynamic overpressure generated in the reaction chamber of the proposed Target Development Facility.

Acknowledgment

This work was supported by Sandia National Laboratories, Albuquerque, NM, under contract 16-9850.

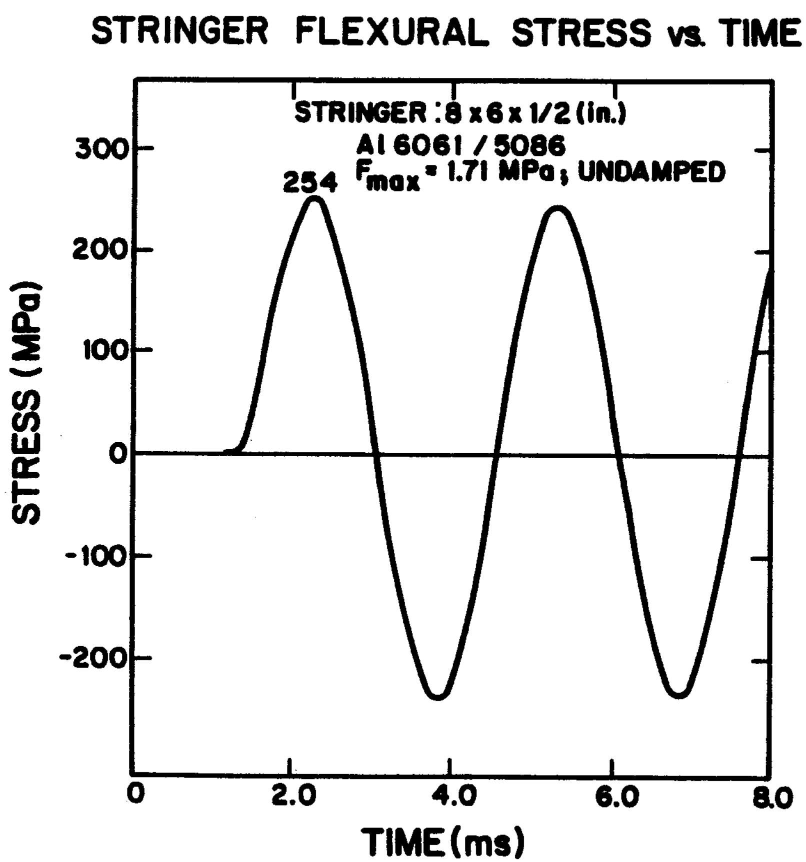

Figure 22

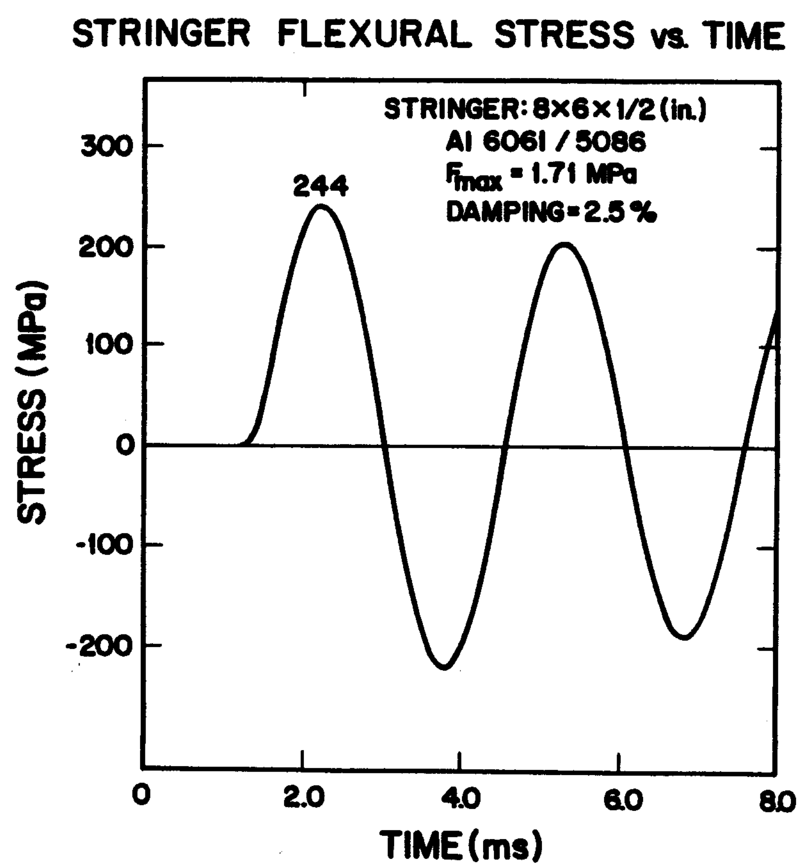

Figure 23

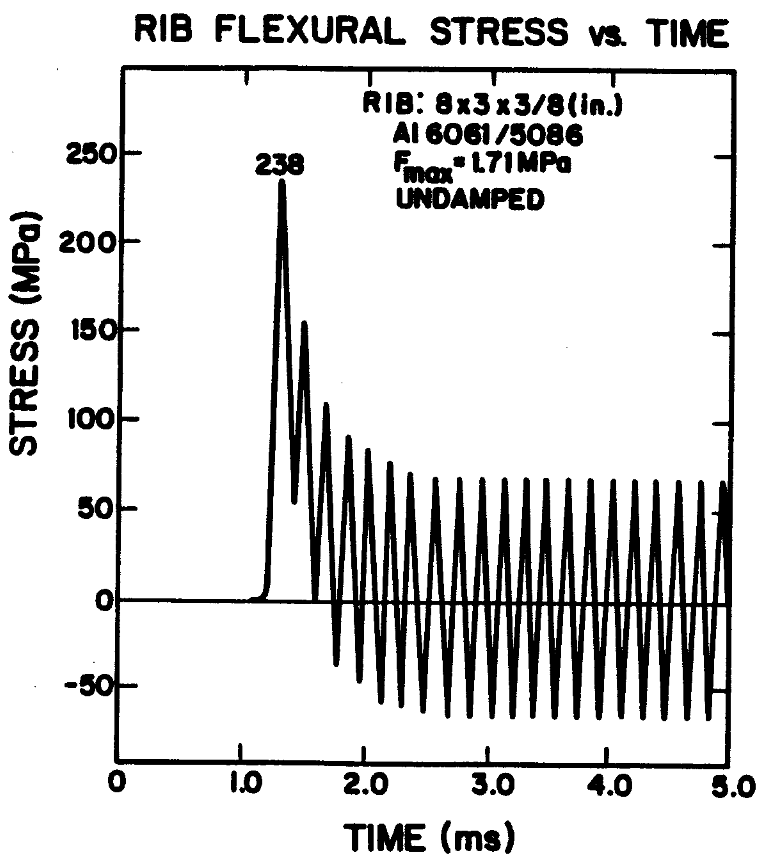

Figure 24

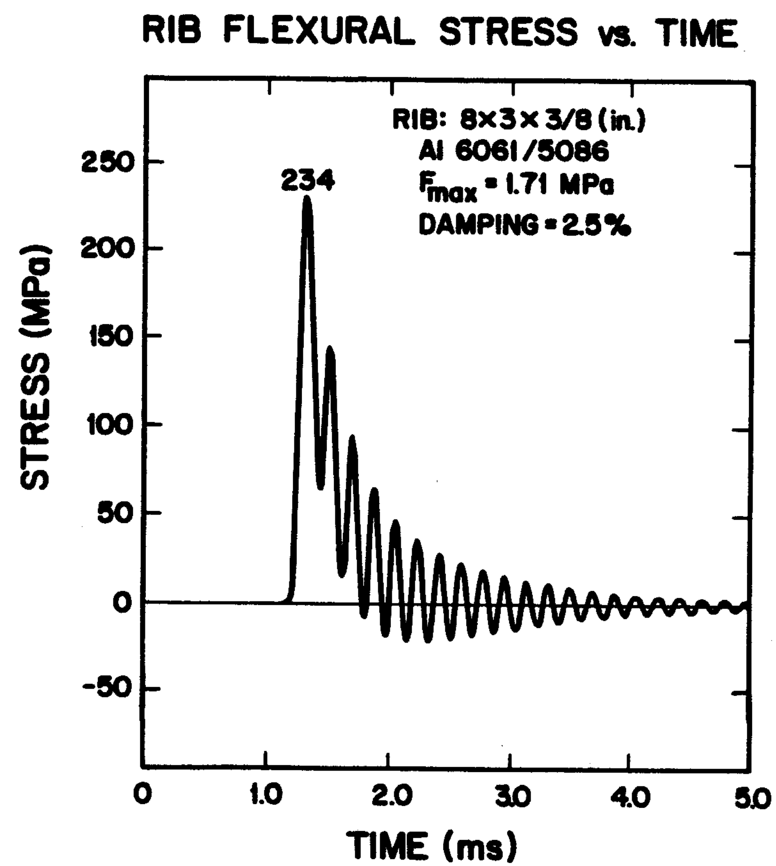

Figure 25

References

1. B. Badger et al., "Report to Sandia Laboratory on University of Wisconsin Fusion Engineering Program Design Activities for the Light Ion Beam Fusion Target Development Facility from August 1981 to February 1982," University of Wisconsin Fusion Engineering Program Report UWFDM-457 (February 1982).

2. R.L. Engelstad and E.G. Lovell, "First Wall Mechanical Design for Light Ion Beam Fusion Reactors," University of Wisconsin Fusion Engineering Program Report UWFDM-322 (December 1979).

3. J.M. Biggs, Introduction to Structural Dynamics, McGraw-Hill, Inc., 1964.

4. R.R. Peterson et al., "Choice of First Wall Material in the Light Ion Beam Target Development Facility," University of Wisconsin Fusion Engineering Program Report UWFDM-456 (February 1982).